ORIGINAL ARTICLE

α-Synuclein reduces acetylserotonin O-methyltransferase mediated melatonin biosynthesis by microtubule-associated protein 1 light chain 3 beta-related degradation pathway

Congcong Jia[1] · Lulu Tian[1] · Cheng Cheng[1] · Jun Zhang[1] · Murad Al-Nusaif[1] · Tianbai Li[1] · Huijia Yang[1] · Yushan Lin[1] · Song Li[1] · Weidong Le[1,2]

Abstract
Previous studies have demonstrated that α-synuclein (α-SYN) is closely associated with rapid eye movement sleep behavior disorder (RBD) related to several neurodegenerative disorders. However, the exact molecular mechanisms are still rarely investigated. In the present study, we found that in the α-SYN[A53T] induced RBD-like behavior mouse model, the melatonin level in the plasma and pineal gland were significantly decreased. To elucidate the underlying mechanism of α-SYN-induced melatonin reduction, we investigated the effect of α-SYN in melatonin biosynthesis. Our findings showed that α-SYN reduced the level and activity of melatonin synthesis enzyme acetylserotonin O-methyltransferase (ASMT) in the pineal gland and in the cell cultures. In addition, we found that microtubule-associated protein 1 light chain 3 beta (LC3B) as an important autophagy adapter is involved in the degradation of ASMT. Immunoprecipitation assays revealed that α-SYN increases the binding between LC3B and ASMT, leading to ASMT degradation and a consequent reduction in melatonin biosynthesis. Collectively, our results demonstrate the molecular mechanisms of α-SYN in melatonin biosynthesis, indicating that melatonin is an important molecule involved in the α-SYN-associated RBD-like behaviors, which may provide a potential therapeutic target for RBD of Parkinson's disease.

Keywords α-Synuclein · Melatonin · ASMT · LC3B · Parkinson's disease

Introduction

Parkinson's disease (PD) is the second most common neurodegenerative disease, affecting 1–4% of the population over 60 years in the world. PD is characterized pathologically by the appearance of Lewy bodies (LBs) in the cytoplasm of surviving neurons [1, 2]. α-Synuclein (α-SYN) and its aggregates are the main components of LBs [3]. The aggregation,

mutation and excessive accumulation of α-SYN reduce the expression of dopamine (DA) neuron-related genes including tyrosine hydroxylase (TH), aromatic L-amino acid decarboxylase (AADC) and solute carrier family 6 member 3 (encoding DA transporter, DAT), thereby affecting the function of DA neurons and causing neurodegeneration [3, 4]. Previous studies have shown that mutants of α-SYN, such as A53T, A30P and E46K, affect the formation of α-SYN fibrils and are associated with autosomal-dominant familial PD [5]. In the transgenic model of PD-like lesions, α-SYN is transferred from the affected neurons to the engrafted neuronal precursor cells and induces the neurons apoptosis [6]. Moreover, the level of α-SYN content in plasma exosome of PD patients is higher than that of healthy controls [7]. The abnormal interaction between α-SYN and TOM20 has also been identified in nigrostriatal neurons of the postmortem PD brain tissue [8]. All these studies indicate the close association between α-SYN and PD.

Sleep disorder is one of the nonmotor symptoms of PD, mostly appeared before motor manifestations occurence

Congcong Jia and Lulu Tian Contributed equally.

✉ Weidong Le
wdle_sibs@163.com

1   Liaoning Provincial Key Laboratory for Research on the Pathogenic Mechanisms of Neurological Diseases, The First Affiliated Hospital, Dalian Medical University, Dalian 116021, China

2   Institute of Neurology, Sichuan Academy of Medical Sciences, Sichuan Provincial Hospital, Chengdu 610072, China

[9–11]. Rapid eye movement (REM) sleep behavior disorder (RBD) is a common sleep disorder and strongly associated with PD. Around half of PD patients have RBD [12, 13]. To explore the RBD pathogenesis of PD, previous studies have constructed different α-SYN pathological models. For instance, Taguchi et al. analyzed nonrapid eye movement (NREM) and REM in A53T SNCA bacterial artificial chromosome transgenic mice (BAC-α-SYN^A53T) and found RBD-like behaviors without any related locomotor dysfunction at 5 months of age [14]. Okuda et al. inoculated α-SYN preformed fibrils (PFFs) into the striatum of BAC-α-SYN^A53T and found that PFFs aggravate REM sleep without atonia [15]. Injection of α-SYN into lateral hypothalamus destroys orexin neurons and induce RBD-like behaviors [16]. Shen et al. injected α-SYN fibers into the lower lateral tegmental nucleus of the brainstem subregion of mice to construct a mouse model with RBD-like behaviors based on α-SYN pathology [17]. Our present study found that prion protein promoter (Prnp) mediated α-SYN^A53T transgenic mice also exhibit RBD-like behaviors at 4–5 months of age preceding motor symptoms. These results suggest that α-SYN pathological models can be used to explore the mechanisms of RBD.

Melatonin is an amine hormone produced by the pineal gland of mammals [13]. Increasing lines of evidence have indicated that melatonin exerts multiple functions in many biological processes, especially in controlling circadian rhythm and improving sleep disorders [18–24]. Kunz et al. have found that the 30-s REM sleep epochs numbers of eight RBD males are significantly reduced by 4 weeks treatment with 3 mg melatonin at night [25]. The clinical symptoms of RBD are absent of a 72-year-old man after melatonin treatment (2 mg a day for 6 months, 30 min before bedtime) [26]. The higher dosages (2–25 mg) of melatonin at night improve sleep efficiency and help reduce secondary sleep disorders, including RBD, indicating the correct administration of melatonin may ameliorate RBD [27, 28]. Besides that, two important catalyzing enzymes have been revealed to be responsible for the biosynthesis of melatonin [29]. The first is N-acetyltransferase (AANAT), which converts serotonin (5-HT) to N-acetyl-5-hydroxytryptamine (NAS). NAS is then metabolized into melatonin by the second enzyme, hydroxyindole-o-methyltransferase (ASMT) [30–32]. This process suggests the possible involvement of AANAT and ASMT in the melatonin-mediated RBD amelioration.

In eukaryotic organisms, maintenance of cellular homeostasis is mediated by two important protein degradation pathways: the ubiquitin–proteasome system (UPS) and autophagy–lysosome pathway (ALP) [33]. In the UPS pathway, the lysine residues of the targeted protein are labeled by ubiquitin (polypeptide) and degraded by the proteasome in a highly specific manner through an energy consuming process [34]. The selective ALP process requires a class of adapter proteins, such as sequestosome 1 (SQSTM1/p62) and ubiquitin-like protein ATG family, to transport the unwanted proteins to the lysosome to complete degradation [35, 36]. In the ALP, light chain 3B (LC3B) is a member of the ATG8 family and is involved in the recruitment of autophagic substrates and autophagosome formation. The consensus LC3-interacting region (LIR) motif (W/F/Y–X–X–L/I/V) of proteins are recognized by LC3B to bind them to promote their degradation [37]. When the autophagy is activated, LC3B is cleaved by ATG4 to generate cytoplasmic LC3B-I. LC3B-I couples phosphatidyl-ethnolamine through ATG7 and ATG3 to produce an LC3B-phosphatidylethanolamine conjugate (LC3B-II), which is a structural protein of autophagy located in the membrane of the autophagic lysosome. In the degradation process, LC3B-II located in the outer membrane of the autophagic lysosome is removed by the cysteine protease ATG4B and recycled, while LC3B-II located in the inner membrane is degraded by lysosome together with the encapsulated content [35, 36].

In this manuscript, we found that α-SYN-reduced melatonin biosynthesis was involved in the α-SYN-associated RBD-like behaviors in vivo. Furthermore, we documented that α-SYN suppressed melatonin biosynthesis through LC3B-mediated ASMT degradation process. Taken together, our studies suggest a LC3B-ASMT pathway underlying the regulating effect of α-SYN on melatonin biosynthesis and provide a potential target for the treatment of RBD in PD.

Materials and methods

Chemicals and antibodies

NAS and Melatonin were purchased from Sigma-Aldrich. Chloroquine, Bafilomycin A1, 3-Methyladenine, Mg132, and Rapamycin were obtained from MedChemExpress. Earle's Balanced Salt Solution was purchased from Beyotime Biotechnology.

The antibodies used in this study were as follows: anti-α-SYN antibody (Santa Cruz Biotechnology and Becton, Dickinson, and Company), anti-ASMT antibody (Novus Biologicals and Genetex), anti-HA magnetic beads and anti-FLAG magnetic beads (MedChemExpress), anti-TH antibody (Millipore), anti-NeuN antibody (Millipore), anti-GAPDH antibody, Goat anti-rabbit Alexa 488 or 594 and Goat anti-mouse Alexa 488 or 594 (Cell Signaling Technology), anti-FLAG, anti-HA (Beyotime Biotechnology), anti-LC3B (Abcam and Cell Signaling Technology), anti-β-Tubulin, Goat anti-rabbit IgG H&L and Goat anti-mouse IgG H&L (Proteintech Group Inc.).

Animals and treatments

B6;C3-Tg(Prnp-human-SNCA*A53T)83Vle/J mice were obtained from the Jackson Laboratory (Stock No: 004479). The heterozygote mice (SNCA*A53T) and wildtype (WT) with the same background were bred to obtain the experimental mice. All the mice were aged 4–5 months during experimentation and housed under a 12:12 light/dark cycle with a constant room temperature and free access to food and water. DNA extracting from the tail of mice was used for genotyping by PCR (2×EasyTaq PCR SuperMix, Transgen Biotechnology Co., Ltd.) with a pair of human SNCA primers. The PCR product of A53T transgenic mice was 417 bp (forward primer: 5′-atggatgtattcatgaaagg-3′, reverse primer: 5′-aggcttcaggttcgtagtcttg-3′) and there was no PCR product in WT mice due to the lack of human SNCA gene expression. The mouse interleukin 2 (IL-2) primers (forward primer: 5′-gagtgccaattcgatgatgagtc-3′, reverse primer: 5′-gcgcttactttgtgctgtccta-3′) were used as a positive control and the PCR product was 407 bp. Tissues of mice with same sex in WT and A53T groups were carried out under deep anesthesia at different zeitgeber times [ZT]. All the animal works were performed according to the guidelines approved by the Animal Care Committee of Dalian Medical University.

Melatonin administration and detection

Transgenic (TG) mice were intraperitoneally injected with melatonin (10 mg/kg/day) for 14 consecutive days at ZT10, and then used to record electroencephalogram/electromyogram (EEG/EMG) data. Whole mouse blood was collected into tubes containing ethylene diamine tetra-acetic acid and then centrifuged at 3000×g for 20 min at 4 ℃. Plasma was collected immediately for assay or stored in aliquot at −80 ℃ for later use. The pineal glands were collected and rinsed with ice-cold phosphate buffered saline (PBS, 0.01 M, pH = 7.4) to remove excess blood thoroughly. Then, the pineal glands were homogenized in PBS containing a protease inhibitor (cocktail, Sigma–Aldrich) and centrifugated for 5 min at 5000×g. Supernatant was collected and melatonin levels were measured by a mouse Melatonin Elisa kit (Cloud-Clone Corp.). Optical density (OD) readings were recorded and melatonin concentrations were calculated by standard curve (generated by CurveExpert 1.3 software).

Mouse behavior tests

Rotarod, open-field and tail suspension tests were performed as described previously [38]. In brief, mice were trained on the rotarod with speed auto accelerating from 4 to 40 r/min in 5 min for 5 consecutive days. The time length of mice stayed on the rotarod was recorded 3 times on day 6 at 1 h intervals. The average time length was used for data analysis. For tail suspension, the mouse's tail was suspended by a tape on a pole (50 cm above the ground) for 6 min, and the cumulative immobile time for the last 4 min was recorded. For open-field test, the mice were placed into 25 × 25 × 30 cm locomotor activity monitor box and recorded the automatic activity for 30 min.

EEG/EMG electrodes implantation, data collection and analysis

Based on the protocols described in our previous studies [39, 40], the mice were fixed on a stereotaxic instrument and continuously anesthetized by inhaling isoflurane. After the skull explosion, four electrodes were fixed at 1.0 mm anterior to bregma, 1.5 mm on both sides; 1.0 mm anterior to the posterior fontanelle, and 1.5 mm on both sides, respectively. Two electromyogram electrodes were inserted into the trapezius muscles on either side. Before testing, all mice were rested for a week and acclimated in the EEG recording room for 3 days. EEG and EMG signals were consecutively recorded for 24 h by a Sirenia EEG acquisition software (Pinnacle Technology Inc.) and the motor activities of animals were monitored by camera. One 24 h period of wake, NREM sleep or REM sleep were determined by visually examining EEG/EMG data within 10 s epochs. Wake stages were characterized by the high amplitude of EMG power and confirmed by cameras videos. A relative increase in the fast Fourier transform (FFT) delta power of EEG amplitudes was used to characterize NREM stages. REM stages were characterized by a relatively low amplitude of EMG power with a relative increase in FFT theta rate (over 70%) [15]. We normalized the REM sleep EMG average values by the same mouse's NREM sleep EMG average values on the same day. To avoid changes in muscle tone caused by alert-phase transitions (such as NREM-REM-NREM or NREM-REM-wake), we included REM periods lasting more than 48 s and eliminated the first and last 8 s during quantization [17].

Pineal organ culture and NAS stimulation

According to the experimental protocol described in previous studies [41, 42]. The pineal glands were rapidly removed from mice and incubated in BGjb medium (Invitrogen) supplemented with antibiotics (penicillin 100 units/mL and streptomycin 100 μg/mL) maintained at 37 ℃, 95% oxygen and 5% carbon dioxide. The pineal gland was cultured for 72 h to denervate and the medium was changed every 24 h.

For NAS stimulation, 200 nM of NAS was added to the medium at ZT3, the pineal glands or cells were collected and the supernatants after homogenization were used to detect the melatonin level after NAS stimulation for 2 h with a mouse Melatonin Elisa kit (Cloud-Clone Corp.).

Cell construction, culture and plasmid transfection

The construction and culture of mouse neuroblastoma N2a cells stably overexpressed with human wildtype α-SYN (WT) or A53T mutant α-SYN (A53T) were described previously [4, 43].

For overexpression of ASMT, we subcloned the coding sequence of mouse ASMT fused with HA tag to pcDNA3.1(-) plasmids. The ASMT-HA plasmid was transfected into N2a cells with lipofectamine 6000 (Beyotime). The cells were screened by 600 µg/mL G418 to obtain the stable cell line with overexpression of ASMT-HA. N2a cells stably overexpressed ASMT-HA were transfected with WT or A53T plasmids with lipofectamine 6000 (Beyotime) for 48 h and then for later use.

Western blot

Cells or the pineal glands of three mice with the same genotype were collected for Western blot (WB). The method of WB was described previously [4, 43]. Briefly, the homogenate supernatant was used to detect the protein concentration by a BCA detection kit (Beyotime) and $5 \times$ sodium dodecyl sulfate (SDS) loading buffer (Beyotime) was added to boil. Equal amounts of total protein were separated by 10–12.5% SDS-polyacrylamide gel electrophoresis (PAGE) and then transferred onto 0.45 µm polyvinylidene difluoride (PVDF) membranes. The membranes were washed, blocked and incubated with the primary antibodies overnight at 4 ℃. Then, the membranes were washed and incubated with the secondary antibody. The protein bands were visualized by the chemiluminescence detection kit (Shanghai Epizyme Biomedical Technology Co., Ltd) and analyzed with the FluorChem Q system (Protein Simple). The intensities of proteins were normalized to GAPDH or β-tubulin, and three experiments were repeated.

Immunofluorescence

Mice were transcardially perfused with 40 mL of ice-cold-PBS at a rate of 10 mL/min after anesthesia. The brain was isolated immediately on ice and fixed with ice-cold 4% paraformaldehyde for 24 h, followed by dehydration in 15% and 30% sucrose. The brain was cut into 40 µm slices by a Leica cryostat (CM1950S, Leica). The whole pineal glands or slices were blocked for 2 h in PBS buffer containing 5% goat serum, 0.2% Triton-X 100 and 0.05% NaN_3 at room temperature and incubated with the primary antibody at 4 ℃ overnight. After washing three times, the slices were stained by the secondary fluorescent antibodies for 1 h at room temperature. Hoechst was used to stain the nucleus.

The images were obtained by A1R MP multiphoton confocal microscope (Nikon). The method of cell immunofluorescence was described previously [4].

Immunoprecipitation

The cell homogenate supernatant was obtained by centrifuging at $12,000 \times g$ at 4 ℃ for 15 min. The protein concentration was determined using a BCA kit (Takara). Equal amount of protein and the primary antibody was added and incubated at 4 ℃ overnight. Then, the protein A/G magnetic beads (MedChemExpress) were added to the protein antibody mixture and incubated at 4 ℃ for 8 h. The protein-antibody-beads mixture was washed with PBS with Tween-20 for three times and boiled at 95 ℃ for 10 min. The protein band was determined by WB.

Liquid chromatography–mass spectrometry

ASMT-HA overexpressed cells were transfected with Vector, WT or A53T plasmid for 48 h with lipofectamine 6000 (Beyotime). The proteins were collected and used to detect the concentration. Equal amount of total protein and HA-magnetic beads (MedChemExpress) were mixed and incubated at 4 ℃ overnight. The protein–HA beads mixture was washed with PBS for five times. The samples underwent enzymolysis, C18 desalting and finally were tested by Q-Exactive plus mass spectrometer (ThermoFisher Scientific).

Statistical analysis

Data were expressed as the mean ± standard deviation (SD). Statistical analyses were performed using GraphPad Prism 8 software (GraphPad prism). Statistical differences between groups were evaluated using independent sample Student's t test or one-way ANOVA. The statistical significance was considered at $P < 0.05$.

Results

Prnp-α-SYN[A53T] transgenic mice exhibit sleep disturbance and RBD-like behaviors at 4–5 months of age without significant motor deficiency

Before evaluating the pathology of Prnp-α-SYN[A53T] TG mice, the body weight of mice was detected after genotyping, the results showed that there was no significant difference between WT and TG (Figure S1A). Then, we analyzed the wake/sleep characteristics of TG mice by recording EEG and EMG. The results showed EEG and EMG differences of sleep/wake structure between WT and TG mice.

The percentages of wake, NREM and REM in WT mice were 64.1, 30.0 and 5.9%, while that in TG mice were 58.2, 37.7 and 4.1%, respectively (Fig. 1A, $P < 0.05$). The ratio of REM to total sleep of TG mice was 40% less than that of WT mice (Fig. 1B, $P < 0.05$). The total REM sleep time of TG mice was 26.3 min less than that of WT mice at 24 h ($P < 0.05$), with separately 19.7 and 6.6 min at the light and dark stages, respectively (Fig. 1C, $P < 0.05$). Moreover, the hourly power density of the REM sleep stage EEG of TG mice was significantly lower than that of WT mice (Fig. 1D), indicating a disrupted sleep quality of TG mice. This result was further verified by the total power density of REM sleep stages (Fig. 1E, $P < 0.05$). In addition, the episode number of TG mice was 48 less than that of WT mice at 24 h ($P < 0.05$), with separately 34 and 14 at light and dark stages,

respectively (Fig. 1F, $P < 0.05$). The average length of REM was not significantly changed in TG mice (Fig. 1G). We then analyzed the integral muscle tone intensity during REM and NREM sleep and found that the EMG_{REM}/EMG_{NREM} ratio of TG mice was significantly higher than that of WT mice (over 74%, Fig. 1H, $P < 0.05$). Finally, we conducted behavioral tests to evaluate motor symptoms in TG mice. The data of rotarod test, tail suspension test and open field test indicated that the behavioral phenotypes of TG mice were not significantly different from that of WT mice (Figure S1B–H). Collectively, these results indicated that TG mice exhibit sleep disturbance and RBD-like behaviors without motor symptoms at 4–5 months of age.

WB analysis and immunofluorescence staining were performed to detect the level of TH, a reliable marker
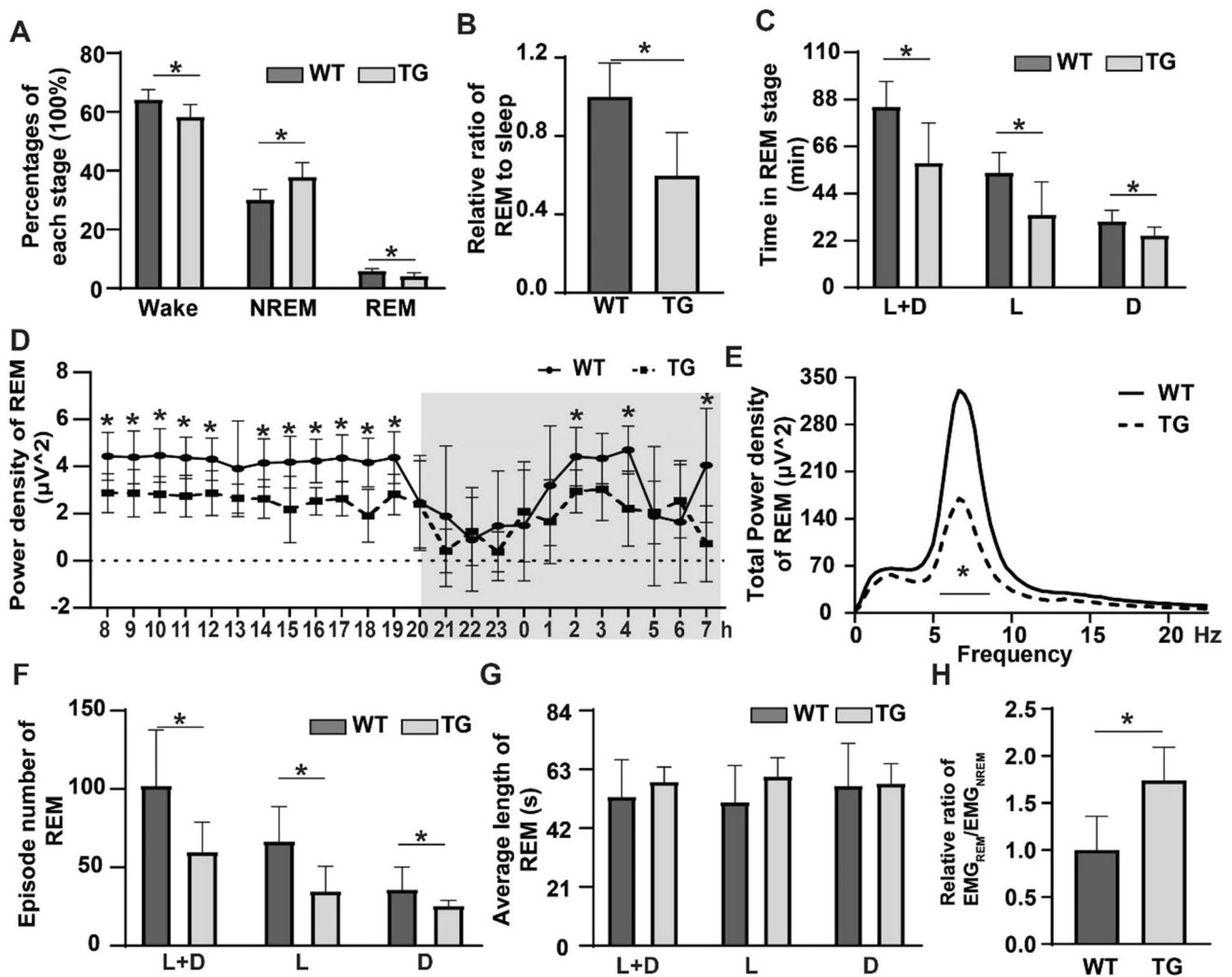

Fig. 1 Sleep structure and RBD-like behaviors in TG mice. **A** The percentages of REM, NREM and wake stages in WT and TG mice. **B** Relative ratio of REM to sleep in 24 h. **C** The total time of REM sleep stages in above mice at 24 h (L+D), light (L) and dark (D). **D** Hourly power density, **E** total power density, **F** episode number and **G** average length of REM stages in WT and TG mice. **H** The relative ratio of EMG_{REM}/EMG_{NREM} in WT and TG mice. $N=5$–7 mice per group. *$P < 0.05$

of dopaminergic neurons, in mouse brain. The results revealed that TH expression in substantia nigra (SN) of TG mice was significantly decreased compared with WT mice in SN (over 40%, Figure S2A, B, E, $P < 0.05$). However, the level of TH in the striatum of TG mice only showed a decreasing trend, without statistical significance compared with WT mice (Figure S2C, D, F).

Melatonin affects α-SYN-induced RBD-like behaviors

To verify the effect of melatonin on α-SYN-induced RBD-like behaviors in TG mice model, we first examined the plasma melatonin level in WT and TG mice at ZT4-6 and ZT10-12. Our results showed that the melatonin levels of TG mice at ZT4-6 and ZT10-12 were 72% and 74% to that of WT mice, respectively (Fig. 2A, $P < 0.05$). Then, we intraperitoneally injected melatonin in TG mice (once
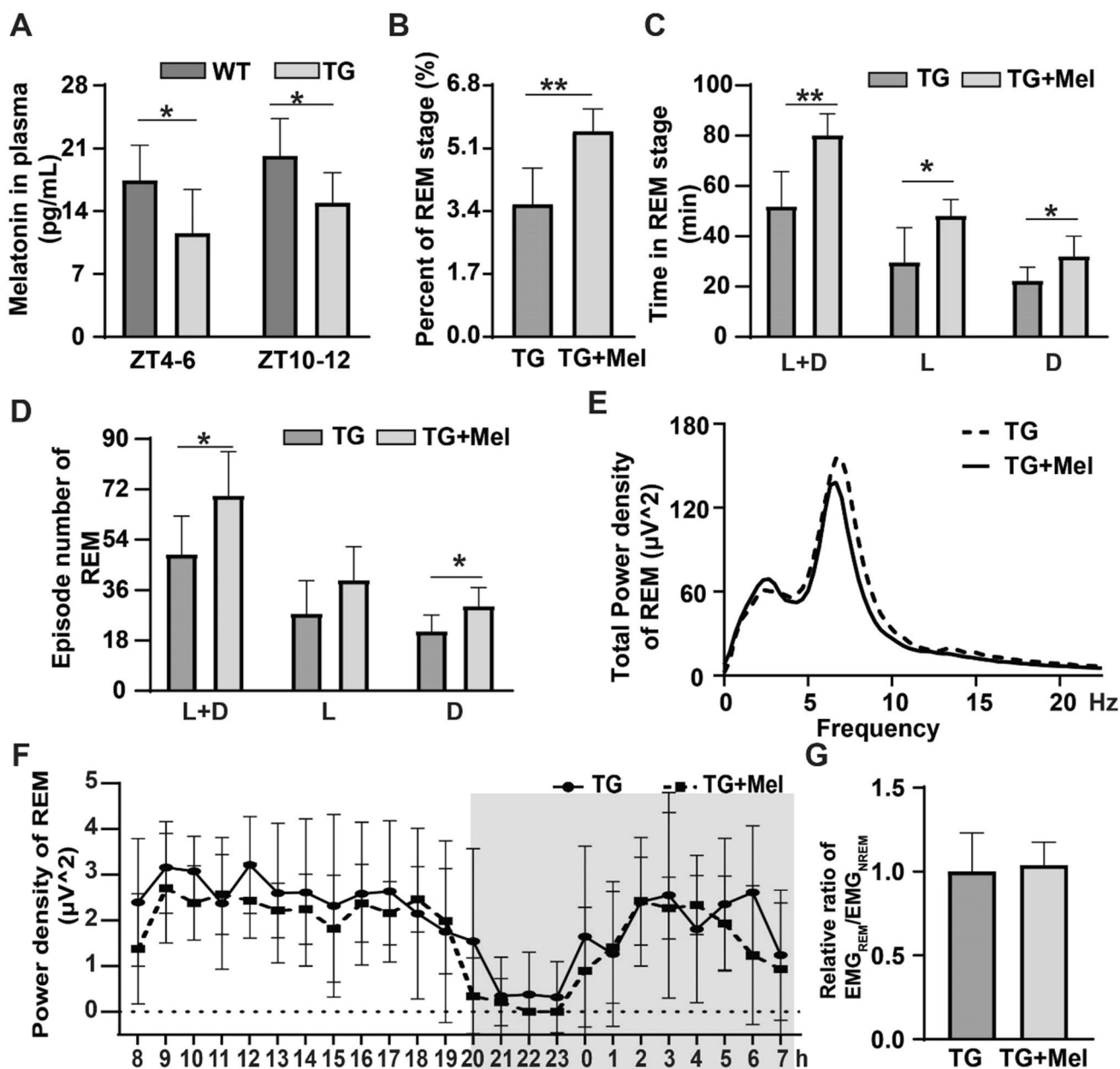
Fig. 2 Melatonin affects α-SYN induced RBD-like behaviors. **A** The plasma melatonin level of WT and TG mice at ZT4-6 and ZT10-12. **B** Percent of REM to sleep in TG and TG injection with melatonin mice (TG+Mel). **C** The total time of REM sleep stages in above mice at 24 h (L+D), light (L) and dark (D). **D** Episode number, **E** total power density and **F** hourly power density of REM in TG and TG+Mel mice. **G** The relative ratio of EMG_{REM}/EMG_{NREM} in TG and TG+Mel mice. $N = 6–9$ mice per group. $*P < 0.05$, $**P < 0.01$

daily for 14 consecutive days) and detected the EEG and EMG of the REM sleep stage of these mice. The results showed that the REM percentage in melatonin-treated TG mice (TG + Mel) was 1.55 folds to that in TG control mice (Fig. 2B, $P < 0.01$). The total REM time of TG + Mel mice was 28.3 min more than that of TG mice at 24 h ($P < 0.01$), containing 18.5 min and 9.8 min at the light and dark stages, respectively (Fig. 2C, $P < 0.05$). In addition, the episode number of TG + Mel mice was 21 more than that of TG control mice at 24 h ($P < 0.05$), with 12 and 19 at the light and dark stages, respectively (Fig. 2D, $P < 0.05$). However, the total, each hour power density of REM and the EMG_{REM}/EMG_{NREM} ratio were not significantly changed by injection of melatonin for a relatively short time (Fig. 2E–G). These

results suggest that melatonin has potential to rescue RBD-like behaviors in TG mice.

α-SYN reduces the expression and activity of ASMT in the pineal gland and in N2a cells

To explore the possible mechanisms underlying the reduced plasma melatonin level in TG mice, we focused on melatonin biosynthesis and detected the melatonin level in the pineal glands. The results showed that the average melatonin level in TG mice at ZT12, 16 and 20 was 35% lower than in WT mice (Fig. 3A, $P < 0.05$), indicating that α-SYN overexpression affected melatonin biosynthesis. Then we examined the protein levels of two melatonin synthases. While AANAT
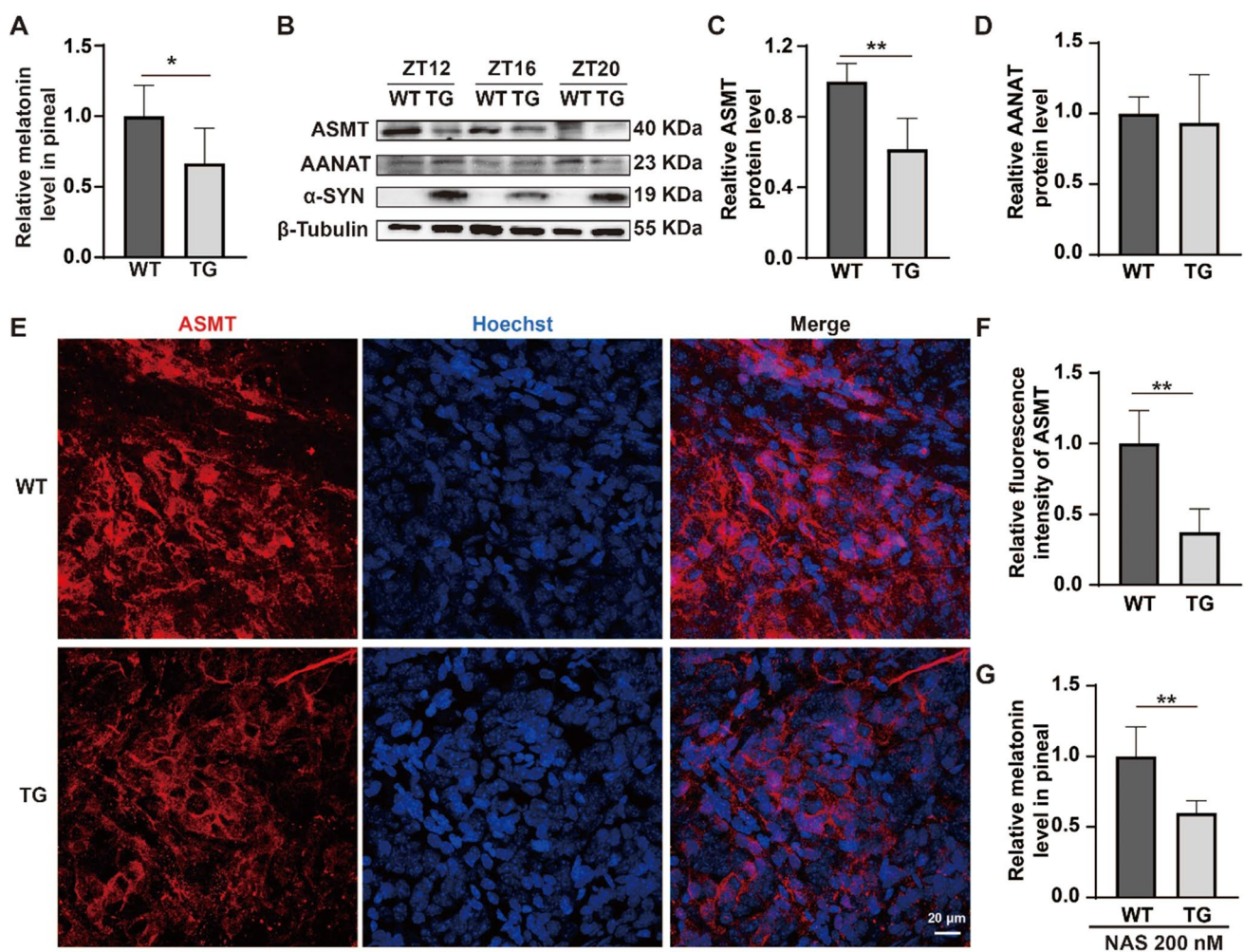
Fig. 3 α-SYN reduces melatonin level and ASMT level and activity in the pineal gland. A Relative melatonin level in the mixture of ZT12, ZT16 and ZT20 pineal glands in WT and TG mice. B The protein level of AANAT and ASMT in the mixture of pineal gland in WT and TG mice at above ZT times. Relative average quantification of C ASMT and D AANAT to β-tubulin (100% WT) in the mixture of pineal glands in WT and TG mice at above ZT times. E Images of ASMT (red) and nucleus stained with Hoechst (blue) in the pineal gland of WT and TG mice at ZT 12. Scale bar: 20 μm. F Relative fluorescence intensity of ASMT in the pineal gland of mice. G Relative melatonin level in the pineal gland of WT and TG mice after NAS (200 nM) stimulation for 2 h in vitro. $N = 4$–9 mice per group. *$P < 0.05$, **$P < 0.01$

expression was not significantly changed in the pineal gland of TG mice at ZT12, 16 and 20 h (Fig. 3B, D), the average expression of ASMT of TG mice at the above ZT times was significantly lower than that of WT mice by 39% (Fig. 3B, C, *P* < 0.01). Immunofluorescence results also confirmed that α-SYN overexpression reduced the ASMT expression level in the pineal gland at ZT12 (Fig. 3E, F, *P* < 0.01). To verify the regulation of α-SYN on ASMT activity, we used NAS to stimulate the pineal gland and detected the new synthesized melatonin level of the pineal gland homogenate. The results showed that the melatonin level of TG mice was 40% less than that of WT mice (Fig. 3G, *P* < 0.01). These results demonstrate that the melatonin synthase ASMT is an important molecular target in α-SYN-induced melatonin reduction.

These results were further confirmed in α-SYN (both WT and A53T) overexpressed cells, as shown by the decreased ASMT levels in both WT and A53T cells (29% and 24% lower compared with control cells, respectively, Fig. 4A, B, *P* < 0.01). Moreover, similar results were also obtained by immunofluorescence staining (Fig. 4C, D, *P* < 0.01). In addition, we also used NAS to stimulate the cells and detected the level of melatonin. The results showed that the melatonin levels of WT and A53T groups were 20% and 26% less than that of the Vector group (Fig. 4E, *P* < 0.01). These results demonstrate that α-SYN mediates the expression level and activity of ASMT, further indicating ASMT is an important molecular target for α-SYN mediated melatonin reduction.

α-SYN promotes LC3B-mediated ASMT degradation

We used α-SYN overexpression cells to investigate the molecular mechanism of α-SYN on ASMT expression. Immunofluorescence staining results showed that α-SYN colocalized with ASMT mainly in the cytoplasm (Figure S3A). Owing to the lack of a recognized mouse ASMT protein antibody for immunoprecipitation, we constructed ASMT-HA overexpression cells (Figure S3B). Then, we transfected WT or A53T plasmids into these cells, and used an anti-HA antibody to pulldown ASMT. Our results showed that ASMT did not have a direct interaction with α-SYN (Figure S3C). The same results were obtained in α-SYN overexpression cells by pulling down α-SYN with an anti-FLAG antibody (Figure S3D). These results demonstrate that ASMT indirectly interacts with α-SYN.

Previous studies indicate that α-SYN induces protein degradation system dysfunction [3, 44, 45]. To determine whether α-SYN affect the degradation of ASMT, we first used CPLM 1.0 (http://cplm.biocuckoo.org/advanced.php) to analyze the association between ASMT and ubiquitin, the results showed that there were no lysine sites to connect with ubiquitin (Figure S4). The protein level of ASMT was also not significantly changed in cells cultured with MG132, a proteasomes inhibitor (Fig. 5A, B), suggesting that ASMT degradation might be independent of the proteasomes system.

Then we used autophagy activators (rapamycin and Earle's Balanced Salt Solution, EBSS) and inhibitors
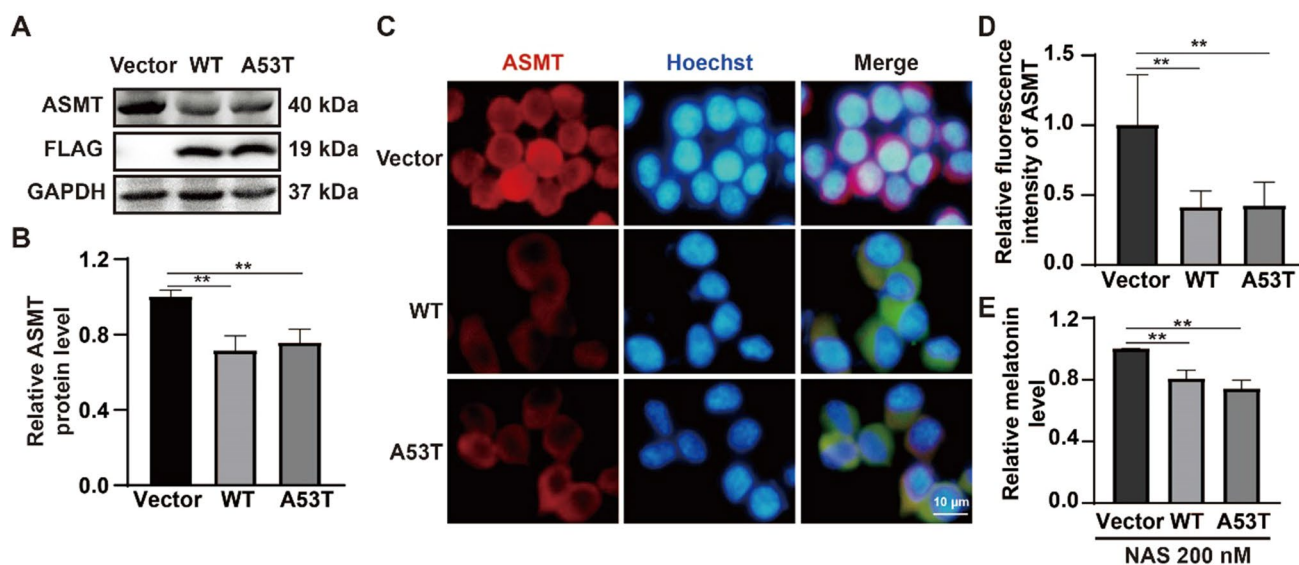
Fig. 4 α-SYN reduces ASMT expression and activity in vitro. **A** The protein level of ASMT in Vector, WT and A53T mouse neuroblastoma N2a cells. **B** Relative quantification of ASMT (F) to GAPDH (100% Vector) in Vector, WT and A53T mouse neuroblastoma N2a cells. **C** Images of ASMT (red), human α-SYN (green) and nucleus stained with Hoechst (blue) in Vector, WT and A53T groups. Scale bar: 20 μm. **D** Relative fluorescence intensity of ASMT in Vector, WT and A53T mouse neuroblastoma N2a cells. **E** Relative melatonin level in Vector, WT and A53T mouse neuroblastoma N2a cells after NAS (200 nM) stimulation for 2 h. *******P* < 0.01
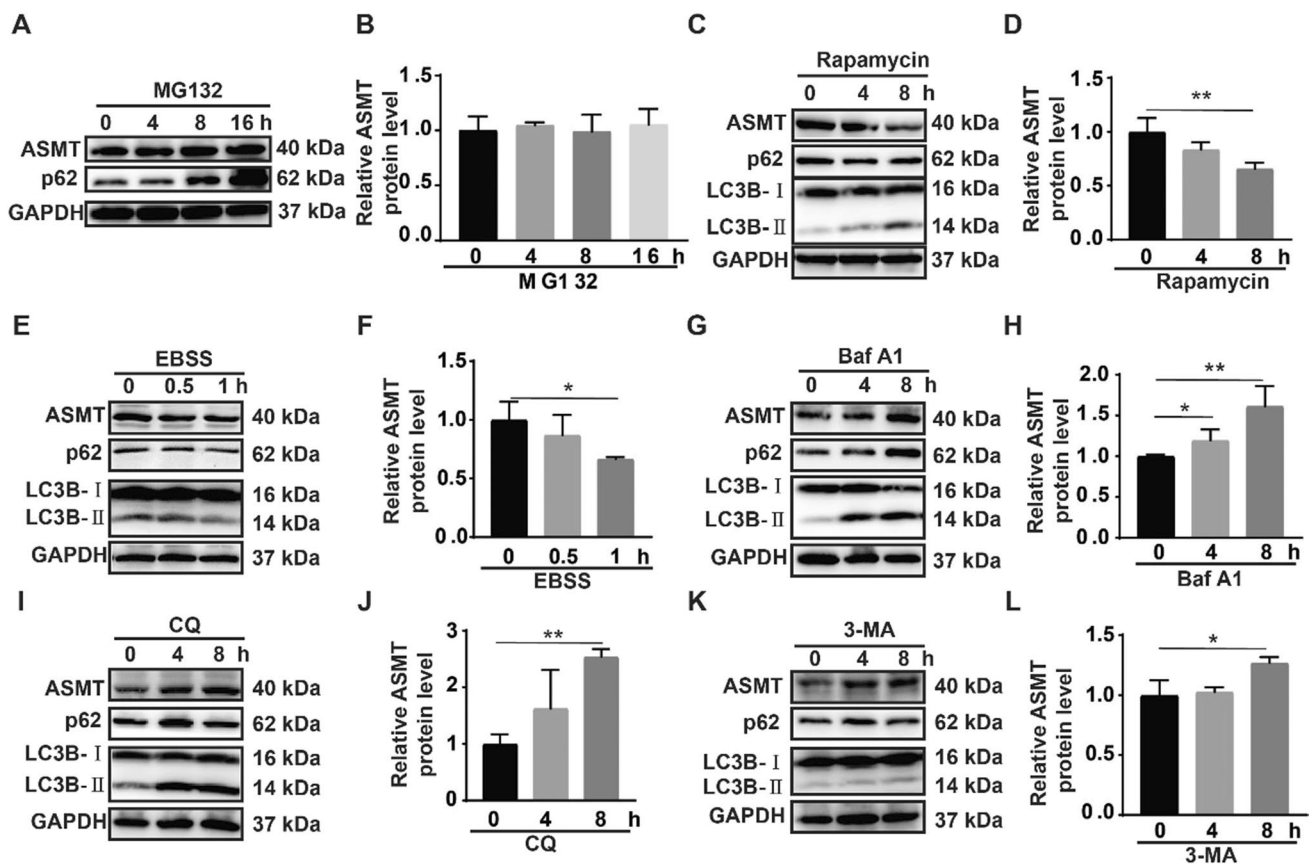
Fig. 5 Autophagy mediates ASMT degradation. **A**, **B** ASMT protein levels and relative quantification of ASMT to GAPDH (100% 0 h) in mouse neuroblastoma N2a cells culture with the proteasome inhibitor MG132 (50 μM) for 0, 4, 8 and 16 h. ASMT protein levels and relative quantification of ASMT to GAPDH (100% 0 h) in mouse neuroblastoma N2a cells culture with the autophagy activator rapamycin (200 nM, **C**, **D**) for 0, 4 and 8 h. ASMT protein levels and relative quantification of ASMT to GAPDH (100% 0 h) in mouse neuroblastoma N2a cells culture with the autophagy activator EBSS for 0, 0.5 and 1 h (**E**, **F**). ASMT protein levels and relative quantification of ASMT to GAPDH (100% 0 h) in mouse neuroblastoma N2a cells culture with the autophagy inhibitors (Bafilomycin A1, Baf A1, 500 nM, **G**, **H**; chloroquine, CQ, 10 μg/mL, **I**, **J**; 3-Methyladenine, 3-MA, 500 μM, **K**, **L**) for 0, 4 and 8 h. *$P < 0.05$, **$P < 0.01$

(chloroquine, CQ; bafilomycin A1, BAF and 3-methyladenine, 3-MA) to treat cell culture for indicated times to explore the effect of autophagy on ASMT degradation. The results showed that rapamycin and EBSS time-dependently reduced the ASMT protein level (Fig. 5C–F), while CQ, BAF and 3-MA increased the ASMT protein level in a time-dependent manner (Fig. 5G–L), indicating autophagy pathway mediates the degradation of ASMT.

Bioinformatics analysis was performed and found that the ASMT protein sequence contains six consensus LC3-interacting region (LIR) motifs (W/F/Y-X-X-L/I/V) that were vital for their binding to LC3B (Fig. 6A). HDOCK software (http://hdock.phys.hust.edu.cn/) [46] analysis also showed a direct interaction between LC3B and ASMT (Fig. 6B). Immunofluorescence staining results further illustrated co-localizations between ASMT and LC3B (Fig. 6C). Moreover, the direct interaction between ASMT and LC3B was verified by immunoprecipitation analysis (Fig. 6D, E) with anti-LC3B or anti-HA antibodies to pulldown the target

protein. Altogether, these data indicated that LC3B is a possible intermediate molecular in α-SYN induced ASMT protein reduction.

To confirm this hypothesis, we used ASMT-HA overexpression cells transfected with WT or A53T plasmids and pulled down ASMT with an anti-HA antibody to detect the binding amount between ASMT and LC3B. The results showed that the binding capacity in WT and A53T cells was 1.4 and 1.5 folds of that in control cells, respectively (Fig. 7A, B, $P < 0.05$ and 0.01, respectively), which was also confirmed by protein mass spectrometry detection (Table S1). Then, we used α-SYN overexpressed cells and pulled down LC3B to detect the binding amount of LC3B with ASMT. The results showed that the binding capacity in WT and A53T cells were increased to 1.2 and 1.2 folds of that in control cells (Fig. 7C, D, $P < 0.05$) and the same results were obtained in immunofluorescence experiments in vitro (Fig. 7E). Moreover, this interaction was further verified using pineal glands, as shown by the increased
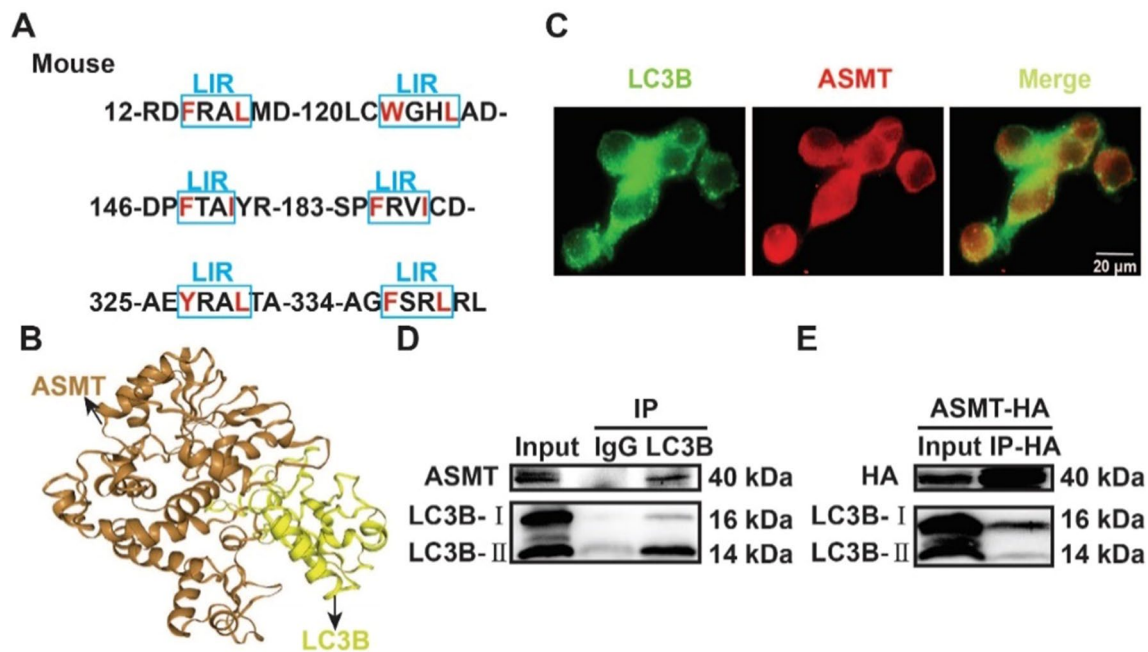
Fig. 6 Direct binding between ASMT and LC3B. **A** Bioinformatics analysis of LIR motifs on ASMT protein sequence and **B** the direct binding between ASMT and LC3B. **C** Images of ASMT (red) and LC3B (green) in mouse neuroblastoma N2a cells. Scale bar: 20 μm.

D Detection of ASMT and LC3B binding by pulling down LC3B in mouse neuroblastoma N2a cells. **E** Detection of ASMT (HA) and LC3B binding by pulling down ASMT using an anti-HA antibody in ASMT-HA overexpressed cells

immunofluorescence co-localization between ASMT and LC3B in TG mice (Fig. 7F). Altogether, α-SYN promotes LC3B-associated ASMT degradation to reduce melatonin synthesis and then affects α-SYN-associated RBD (Fig. 8).

Discussion

Sleep disorder is a nonmotor symptom occurring not only in the late stage, but also in the early stage of PD [47]. Consistent with this, our results showed that at 4–5 months of age, Prnp-human-α-SYN^{A53T} transgenic mice did not exhibit motor symptoms but appeared to have sleep disorders (Figure S1, 1). REM, an important stage of sleep, plays an important role in cleaning up brain toxins, promoting brain growth and development, regulating cognition and emotions [48, 49]. It is of great importance to explore the causes of RBD and find effective treatment strategies to alleviate RBD and then improve the life quality of PD patients. In this study, our results demonstrate that α-SYN^{A53T} transgenic mice exhibit RBD-like behaviors at 4–5 months of age, as evidenced by the decreased time, power density episode number and increased REM/NREM EMG variance ratio (Fig. 1). The same results in different α-SYN-associated PD models have been shown in others studies. For instance, REM sleep without atonia was exhibited in BAC-α-SYN transgenic mice at 5 months of age [14], and inoculation into

the striatum of above mice with α-SYN preformed fibrils aggravated REM sleep without atonia after 1 month [15]. Injection of α-SYN fibrils into the sublaterodorsal tegmental nucleus induces RBD-like behaviors in mice [17]. Our results declare that Prnp-human-α-SYN^{A53T} transgenic mice also can be used as RBD-like behaviors models to further explore the causes and treatment for RBD of PD.

Melatonin is synthesized in the pineal gland of mammals, with low levels during the day and high level at night [50], and altered in neurodegenerative diseases. Previous studies of our and others' have shown that the plasma melatonin level of PD patients was lower compared with healthy controls [11, 51]. Consistent with this, TG mice had reduced plasma melatonin level compared with WT mice in this study (Fig. 2A). Additionally, melatonin is a regulator of circadian rhythm that plays an important role in regulating sleep wake cycles and involved in various sleep disorders, including RBD [52, 53]. Kunz et al. have shown that the RBD symptom of patients are severity improved over the first 4 weeks of treatment of melatonin (2 mg one day at night) [54]. Treatment with 3 mg melatonin at night for 4 weeks reduce the number of 30-s REM sleep epochs of eight RBD males [25]. In the present study, we injected melatonin in TG transgenic mice at night for a relatively short time, and the results showed that melatonin increased the stage time and episode number of REM (Fig. 2), demonstrating that melatonin can alleviate α-SYN induced RBD
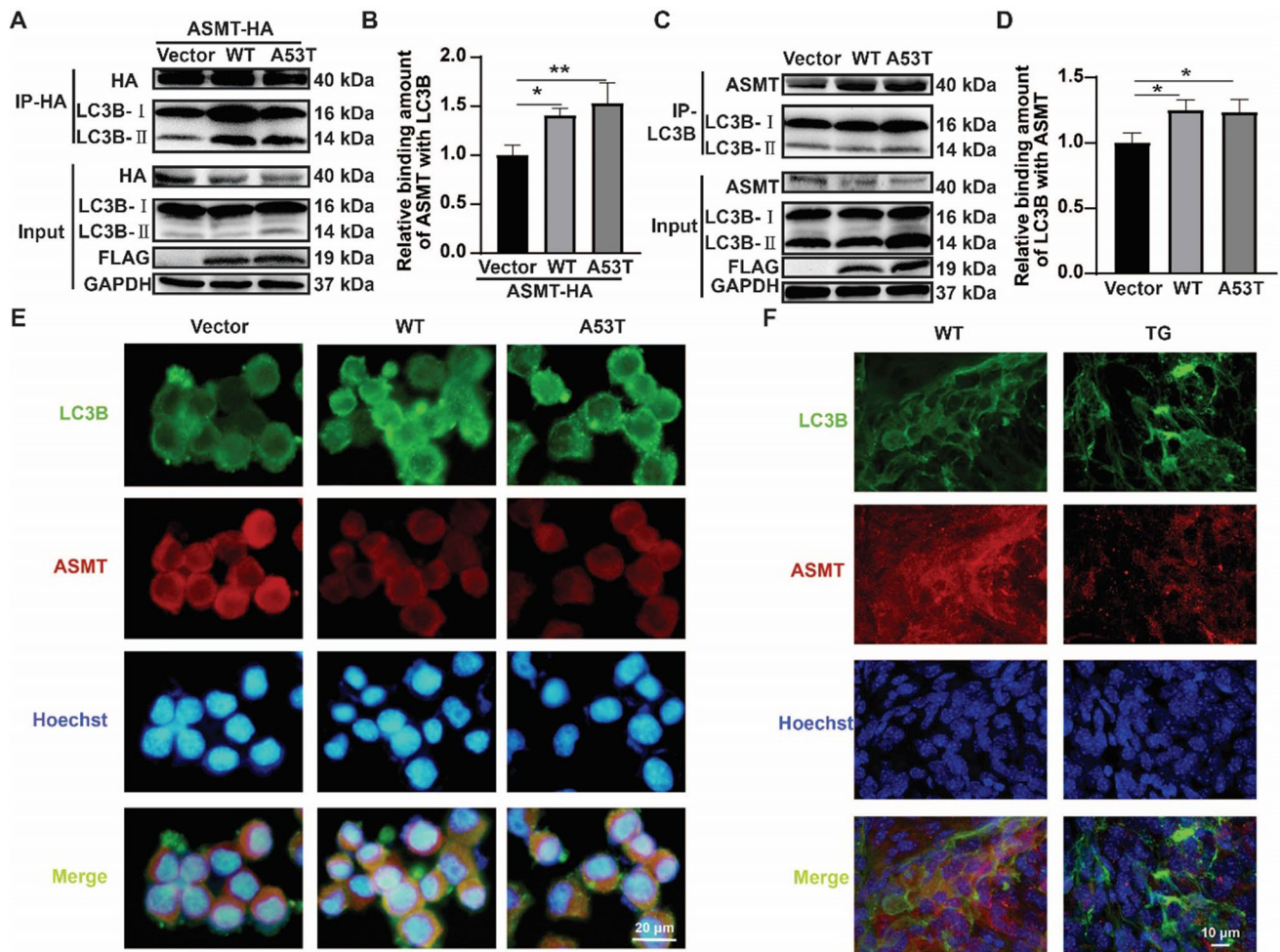
Fig. 7 α-Syn affects the binding amount between ASMT and LC3B. **A**, **B** Western blot detection of the binding amount between LC3B and ASMT (HA) and relative quantification of LC3B to HA (100% Vector) by pulling down ASMT with an anti-HA antibody in ASMT overexpressed mouse neuroblastoma N2a cells transfected with Vector, WT and A53T plasmids. **C**, **D** Western blot detection of the binding amount between LC3B and ASMT and relative quantification of ASMT to LC3B (100% Vector) by pulling down LC3B in Vector, WT and A53T mouse neuroblastoma N2a cells. **E** Images of ASMT (red), LC3B (green) and nucleus stained with Hoechst (blue) in Vector, WT and A53T cells. Scale bar: 20 μm. **F** Images of ASMT (red), LC3B (green) and nucleus stained with Hoechst (blue) in pineal gland of WT and TG mice at ZT 12. Scale bar: 10 μm. *$P < 0.05$, **$P < 0.01$

Fig. 8 The schematic diagram of this study. Overexpression of α-SYN promotes LC3B mediated ASMT degradation to reduce melatonin biosynthesis and then affects RBD-like behaviors
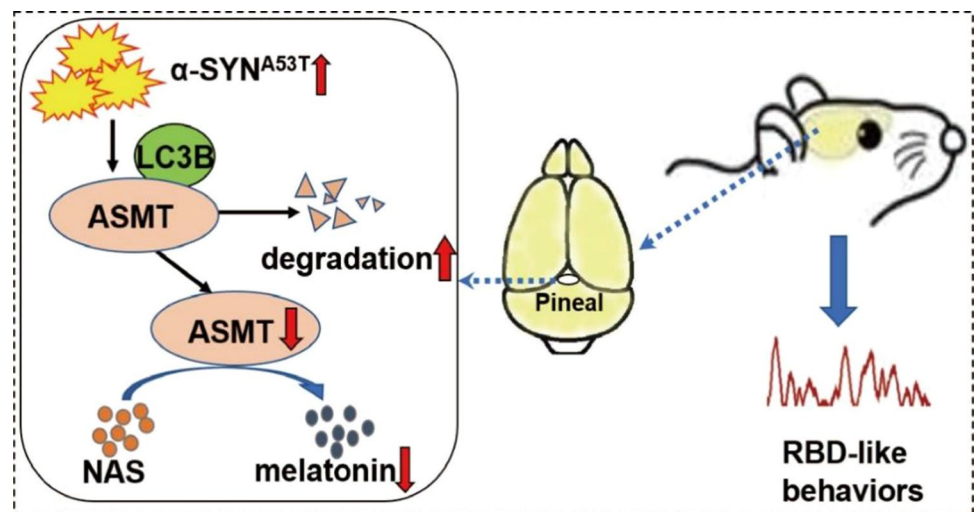
to a certain extent and melatonin is a crucial molecule in α-SYN induced RBD-like behaviors. One possible reason of this mitigative effect is that injection of melatonin reduces the toxic α-SYN in the important RBD brain tissues. We detected the melatonin level and the α-SYN level in the circadian clock regulation center (hypothalamus), the results showed that melatonin is decreased in the hypothalamus of TG mice, which can be increased after injection of melatonin. While the protein level of α-SYN is nearly unchanged before or after injection of melatonin. These results tend to that the changed RBD-like behaviors in TG mice after melatonin injection are a result from a rescuing effect of melatonin. However, these results in other important RBD brain tissues remain to be further explored.

One mechanism of melatonin improves sleep disorder is via activating two high affinity G protein coupled receptors (MT1 and MT2) [55]. MT1 receptors are located in the locus coeruleus and lateral hypothalamus associated with REM sleep [56], while MT2 receptors are in the reticular thalamus associated with NREM sleep [57]. The different localizations between MT1 and MT2 receptors determine their different roles in modulating sleep. Recent studies showed that the activation of the MT1 receptor is mainly involved in the regulation of REM sleep, while the MT2 receptor selectively increases NREM sleep [58, 59]. Besides that, a decrease NREM sleep stage is observed in MT2 receptor knockout mice, whereas an increased NREM sleep stage and a decrease REM sleep stage are revealed in MT1 receptor knockout mice [57, 60]. Our results showed that both melatonin and MT1 levels are downregulated in the hypothalamus of A53T TG mice, indicating MT1 is a potential intermediate molecular in the α-SYN-melatonin-related RBD pathway. In addition, melatonin is involved in antioxidant, anti-inflammatory, antiapoptotic and circadian functions by regulating many molecules [61], providing that the possible mechanism of melatonin in the α-SYN-induced RBD-like behaviors.

Although melatonin affects the α-SYN induced RBD-like behaviors, the photo-instability of melatonin determines its limitations in the induction of these behaviors, indicating that there may be other important molecules in the process. For instance, the hypocretin neurons control motor during wakefulness and sleep in humans, their deficiency induces a motor control defect during REM sleep [62]. Injection of α-SYN into the lateral hypothalamus area decreases hypocretin receptor 1 (OX1R)-mediated signaling associated with RBD occurrence [16]. Moreover, gene blocking of GABA and glycine receptors increases muscle twitches during REM sleep [63]. Intrastriatal injection of α-SYN fibrils reduce septal GABAergic neurons, indicating GABAergic neurons maybe the intermediate molecules in the pathway of α-SYN induced RBD-like behaviors [64]. The abnormal expression level and dysfunction of biological rhythm genes (the circadian locomotor output cycle kaput, Clock, brain and muscle aryl-hydrocarbon receptor nuclear translocator-like 1, Bmal1, Period 1, Per1, Period 2, Per2, Period 3, Per3 and cryptochrome 1, Cry 1 and cryptochrome 2, Cry 2) induce circadian rhythm sleep–wake disorders [65]. Bmal1 expression is lack of time-dependent changes in PD patients with decreased REM sleep, indicating the rhythm genes are also an important molecular in the α-SYN induced RBD-like behaviors [11]. Molecules that regulate rhythm genes may be potential mediators of α-SYN induced RBD-like behaviors, which still need to further exploration.

We demonstrated that only the ASMT protein level was reduced in TG mice (Fig. 3B–D), indicating the low melatonin level of TG mice is partially due to deficient biosynthesis (Fig. 3A). The proteasome system is an important protein degradation system to control the protein quality of the body in PD [33]. A previous study has shown that α-SYN promotes the proteasome dependent degradation of Nurr1 by treating the midbrain cultures of TG and littermate control mice with MG132 [3]. In the rat substantia nigra pars compacta co-expressed with α-SYN^A53T and the ubiquitinated reporter protein UbG76V-GFP by adeno-associated viruses, the early-onset catalytic injury of the 26S proteasome with associated ubiquitin–proteasome system (UPS) dysfunction is induced by overexpression of α-SYN [66]. Although α-SYN mediates the function of the proteasome system, the regulation of α-SYN on ASMT expression is independent of the UPS system due to no lysine sites connected with ubiquitin in the ASMT protein sequence (Figure S4).

Autophagy is another critical process for protein homeostasis in eukaryotic cells [67], and many compounds have been explored as inhibitors or agonists of autophagy function [33]. In this study we determined whether autophagy participates in ASMT degradation, showing that higher autophagic activity decreased ASMT protein level, while autophagy inhibition increased ASMT protein level (Fig. 5C–L). LC3B as an autophagy marker plays an important role in autophagosome formation and autophagy's substrate recruitment. In the process of autophagy mediated protein degradation, LC3B recognizes the LIR motifs of protein, and cytoplasmic LC3B (LC3B-I) is enzymatically hydrolyzed a small segment of polypeptide and transformed to membrane type (LC3B-II) [35, 68]. Our bioinformatics analysis showed that the ASMT protein sequence has six LIR motifs binding to LC3B, which can be verified by immunofluorescence and immunoprecipitation results (Fig. 6), indicating LC3B mediated the degradation of ASMT. However, the specific binding sites of ASMT to LC3B and the effect of α-SYN on these sites still need further exploration.

In the transgenic mice model expressing PITX3/ H2BjGFP/A53T, LC3B positive puncta exhibited increased size and intensity in the soma of mDA neurons at one month of age. In addition, a significant increase

in LC3B protein level was observed in the midbrain [3]. Dehay et al. have found that LC3B-II was increased in the SN of PD models [69]. In our study, LC3B protein level was also increased in the pineal gland of TG mice without significantly morphological changes, and α-SYN increased the combination between ASMT and LC3B (Fig. 7), thus promoting the degradation of ASMT. These results confirm the previous findings that α-SYN regulates autophagy-dependent degradation pathways, which provide a potential molecular mechanism underlying the effects of α-SYN on ASMT expression and function [3, 70].

In summary, our study documented a new α-SYN-based RBD-like behaviors model and the potential molecular mechanism underlying the α-SYN-reduced expression and activity of ASMT through LC3B-associated degradation pathway. The impaired ASMT-mediated melatonin synthesis by α-SYN may help to understand the molecular mechanism of RBD-like behaviors in α-SYN-based transgenic mice, providing a new therapeutic target for the treatment of this disease.

Data availability The data used and /or analyzed during the present study are available from the corresponding author on reasonable request.

Declarations

Conflict of interests The authors have no relevant financial or non-financial interests to disclose.

Ethics approval Animal care and procedures were carried out in accordance with the Laboratory Animal Care Guidelines approved by the Institutional Animal Care Committee at Dalian Medical University. The protocol was approved by the Institutional Animal Care Committee at Dalian Medical University (approval number AEE19022).

Consent to participate Not applicable.

Consent to publish Not applicable.

References

1. Lees AJ, Hardy J, Revesz T (2009) Parkinson's disease. Lancet 373:2055–2066. https://doi.org/10.1016/S0140-6736(09)60492-X

2. Przedborski S (2017) The two-century journey of Parkinson disease research. Nat Rev Neurosci 18:251–259. https://doi.org/10.1038/nrn.2017.25

3. Lin X, Parisiadou L, Sgobio C, Liu G, Yu J, Sun L, Shim H, Gu XL, Luo J, Long CX, Ding J, Mateo Y, Sullivan PH, Wu LG, Goldstein DS, Lovinger D, Cai H (2012) Conditional expression of Parkinson's disease-related mutant alpha-synuclein in the midbrain dopaminergic neurons causes progressive neurodegeneration and degradation of transcription factor nuclear receptor related 1. J Neurosci 32:9248–9264. https://doi.org/10.1523/JNEUROSCI.1731-12.2012

4. Jia C, Qi H, Cheng C, Wu X, Yang Z, Cai H, Chen S, Le W (2020) Alpha-synuclein negatively regulates Nurr1 expression through NF-kappaB-related mechanism. Front Mol Neurosci 13:64. https://doi.org/10.3389/fnmol.2020.00064

5. Dev KK, Hofele K, Barbieri S, Buchman VL, van der Putten H (2003) Part II: alpha-synuclein and its molecular pathophysiological role in neurodegenerative disease. Neuropharmacology 45:14–44. https://doi.org/10.1016/s0028-3908(03)00140-0

6. Desplats P, Lee HJ, Bae EJ, Patrick C, Rockenstein E, Crews L, Spencer B, Masliah E, Lee SJ (2009) Inclusion formation and neuronal cell death through neuron-to-neuron transmission of alpha-synuclein. Proc Natl Acad Sci U S A 106:13010–13015. https://doi.org/10.1073/pnas.0903691106

7. Shi M, Liu C, Cook TJ, Bullock KM, Zhao Y, Ginghina C, Li Y, Aro P, Dator R, He C, Hipp MJ, Zabetian CP, Peskind ER, Hu SC, Quinn JF, Galasko DR, Banks WA, Zhang J (2014) Plasma exosomal alpha-synuclein is likely CNS-derived and increased in Parkinson's disease. Acta Neuropathol 128:639–650. https://doi.org/10.1007/s00401-014-1314-y

8. Di Maio R, Barrett PJ, Hoffman EK, Barrett CW, Zharikov A, Borah A, Hu X, McCoy J, Chu CT, Burton EA, Hastings TG, Greenamyre JT (2016) Alpha-Synuclein binds to TOM20 and inhibits mitochondrial protein import in Parkinson's disease. Sci Transl Med. 8:342ra378. https://doi.org/10.1126/scitranslmed.aaf3634

9. Chaudhuri KR, Healy DG, Schapira AH, National Institute for Clinical E (2006) Non-motor symptoms of Parkinson's disease: diagnosis and management. Lancet Neurol 5:235–245. https://doi.org/10.1016/S1474-4422(06)70373-8

10. Salawu FK, Danburam A, Olokoba AB (2010) Non-motor symptoms of Parkinson's disease: diagnosis and management. Niger J Med 19:126–131. https://doi.org/10.4314/njm.v19i2.56496

11. Breen DP, Vuono R, Nawarathna U, Fisher K, Shneerson JM, Reddy AB, Barker RA (2014) Sleep and circadian rhythm regulation in early Parkinson disease. JAMA Neurol 71:589–595. https://doi.org/10.1001/jamaneurol.2014.65

12. Zhang F, Niu L, Liu X, Liu Y, Li S, Yu H, Le W (2020) Rapid eye movement sleep behavior disorder and neurodegenerative diseases: an update. Aging Dis 11:315–326. https://doi.org/10.14336/AD.2019.0324

13. Zhang X, Sun X, Wang J, Tang L, Xie A (2017) Prevalence of rapid eye movement sleep behavior disorder (RBD) in Parkinson's disease: a meta and meta-regression analysis. Neurol Sci 38:163–170. https://doi.org/10.1007/s10072-016-2744-1

14. Taguchi T, Ikuno M, Hondo M, Parajuli LK, Taguchi K, Ueda J, Sawamura M, Okuda S, Nakanishi E, Hara J, Uemura N, Hatanaka Y, Ayaki T, Matsuzawa S, Tanaka M, El-Agnaf OMA, Koike M, Yanagisawa M, Uemura MT, Yamakado H, Takahashi R (2020) Alpha-Synuclein BAC transgenic mice exhibit

RBD-like behaviour and hyposmia: a prodromal Parkinson's disease model. Brain 143:249–265. https://doi.org/10.1093/brain/awz380

15. Okuda S, Nakayama T, Uemura N, Hikawa R, Ikuno M, Yamakado H, Inoue H, Tachibana N, Hayashi Y, Takahashi R, Egawa N (2022) Striatal-inoculation of alpha-synuclein preformed fibrils aggravated the phenotypes of REM sleep without atonia in A53T BAC-SNCA transgenic mice. Int J Mol Sci 23:13390. https://doi.org/10.3390/ijms232113390

16. Fan JK, Wang MC, Yang HM, Zhang JN, Gu L, Zhang H (2023) Alpha-synuclein induced the occurrence of RBD via interaction with OX1R and modulated its degradation. Neuromolecular Med. https://doi.org/10.1007/s12017-023-08735-4

17. Shen Y, Yu WB, Shen B, Dong H, Zhao J, Tang YL, Fan Y, Yang YF, Sun YM, Luo SS, Chen C, Liu FT, Wu JJ, Xiao BG, Yu H, Koprich JB, Huang ZL, Wang J (2020) Propagated alpha-synucleinopathy recapitulates REM sleep behaviour disorder followed by parkinsonian phenotypes in mice. Brain 143:3374–3392. https://doi.org/10.1093/brain/awaa283

18. Reiter RJ (1993) The melatonin rhythm: both a clock and a calendar. Experientia 49:654–664. https://doi.org/10.1007/BF01923947

19. Jilg A, Bechstein P, Saade A, Dick M, Li TX, Tosini G, Rami A, Zemmar A, Stehle JH (2019) Melatonin modulates daytime-dependent synaptic plasticity and learning efficiency. J Pineal Res 66:e12553. https://doi.org/10.1111/jpi.12553

20. Ahmad SB, Ali A, Bilal M, Rashid SM, Wani AB, Bhat RR, Rehman MU (2023) Melatonin and health: insights of melatonin action, biological functions, and associated disorders. Cell Mol Neurobiol 43:2437–2458. https://doi.org/10.1007/s10571-023-01324-w

21. Fernandez A, Ordonez R, Reiter RJ, Gonzalez-Gallego J, Mauriz JL (2015) Melatonin and endoplasmic reticulum stress: relation to autophagy and apoptosis. J Pineal Res 59:292–307. https://doi.org/10.1111/jpi.12264

22. Galano A, Tan DX, Reiter RJ (2011) Melatonin as a natural ally against oxidative stress: a physicochemical examination. J Pineal Res 51:1–16. https://doi.org/10.1111/j.1600-079X.2011.00916.x

23. Su LY, Liu Q, Jiao L, Yao YG (2021) Molecular mechanism of neuroprotective effect of melatonin on morphine addiction and analgesic tolerance: an update. Mol Neurobiol 58:4628–4638. https://doi.org/10.1007/s12035-021-02448-0

24. Qin DZ, Cai H, He C, Yang DH, Sun J, He WL, Li BL, Hua JL, Peng S (2021) Melatonin relieves heat-induced spermatocyte apoptosis in mouse testes by inhibition of ATF6 and PERK signaling pathways. Zool Res 42:514–524. https://doi.org/10.24272/j.issn.2095-8137.2021.041

25. Kunz D, Mahlberg R (2010) A two-part, double-blind, placebo-controlled trial of exogenous melatonin in REM sleep behaviour disorder. J Sleep Res 19:591–596. https://doi.org/10.1111/j.1365-2869.2010.00848.x

26. Kunz D, Bes F (2017) Twenty years after: another case report of melatonin effects on REM sleep behavior disorder, using serial dopamine transporter imaging. Neuropsychobiology 76:100–104. https://doi.org/10.1159/000488893

27. Auld F, Maschauer EL, Morrison I, Skene DJ, Riha RL (2017) Evidence for the efficacy of melatonin in the treatment of primary adult sleep disorders. Sleep Med Rev 34:10–22. https://doi.org/10.1016/j.smrv.2016.06.005

28. Kunz D (2013) Melatonin in rapid eye movement sleep behavior disorder: why does it work? Sleep Med 14:705–706. https://doi.org/10.1016/j.sleep.2013.05.004

29. Ebihara S, Marks T, Hudson DJ, Menaker M (1986) Genetic control of melatonin synthesis in the pineal gland of the mouse. Science 231:491–493. https://doi.org/10.1126/science.3941912

30. Reiter RJ (1991) Pineal melatonin: cell biology of its synthesis and of its physiological interactions. Endocr Rev 12:151–180. https://doi.org/10.1210/edrv-12-2-151

31. Axelrod J, Weissbach H (1960) Enzymatic O-methylation of N-acetylserotonin to melatonin. Science 131:1312. https://doi.org/10.1126/science.131.3409.1312

32. Juhnevica-Radenkova K, Moreno DA, Ikase L, Drudze I, Radenkovs V (2020) Naturally occurring melatonin: sources and possible ways of its biosynthesis. Compr Rev Food Sci Food Saf 19:4008–4030. https://doi.org/10.1111/1541-4337.12639

33. Dikic I (2017) Proteasomal and autophagic degradation systems. Annu Rev Biochem 86:193–224. https://doi.org/10.1146/annurev-biochem-061516-044908

34. Finley D (2009) Recognition and processing of ubiquitin-protein conjugates by the proteasome. Annu Rev Biochem 78:477–513. https://doi.org/10.1146/annurev.biochem.78.081507.101607

35. Lamb CA, Yoshimori T, Tooze SA (2013) The autophagosome: origins unknown, biogenesis complex. Nat Rev Mol Cell Biol 14:759–774. https://doi.org/10.1038/nrm3696

36. Klionsky DJ, Abdel-Aziz AK, Abdelfatah S, Abdellatif M, Abdoli A, Abel S, Abeliovich H, Abildgaard MH, Abudu YP, Acevedo-Arozena A, Adamopoulos IE, Adeli K, Adolph TE, Adornetto A, Aflaki E, Agam G, Agarwal A, Aggarwal BB, Agnello M, Agostinis P, Tong CK (2021) Guidelines for the use and interpretation of assays for monitoring autophagy (4th edition)1. Autophagy 17:1–382. https://doi.org/10.1080/15548627.2020.1797280

37. Kraft LJ, Nguyen TA, Vogel SS, Kenworthy AK (2014) Size, stoichiometry, and organization of soluble LC3-associated complexes. Autophagy 10:861–877. https://doi.org/10.4161/auto.28175

38. Wang P, Chen X, Wang Y, Jia C, Liu X, Wang Y, Wu H, Cai H, Shen HM, Le W (2021) Essential role for autophagy protein VMP1 in maintaining neuronal homeostasis and preventing axonal degeneration. Cell Death Dis 12:116. https://doi.org/10.1038/s41419-021-03412-5

39. Zhang F, Zhong R, Li S, Fu Z, Wang R, Wang T, Huang Z, Le W (2019) Alteration in sleep architecture and electroencephalogram as an early sign of Alzheimer's disease preceding the disease pathology and cognitive decline. Alzheimers Dement 15:590–597. https://doi.org/10.1016/j.jalz.2018.12.004

40. Liu X, Yu H, Wang Y, Li S, Cheng C, Al-Nusaif M, Le W (2022) Altered motor performance, sleep EEG, and Parkinson's disease pathology induced by chronic sleep deprivation in Lrrk 2(G2019S) Mice. Neurosci Bull 38:1170–1182. https://doi.org/10.1007/s12264-022-00881-2

41. Chansard M, Liang J, Iwahana E, Baker T, Whittaker J, Fukuhara C (2006) Role of calcium in the gating of isoproterenol-induced arylalkylamine N-acetyltransferase gene expression in the mouse pineal gland. J Pineal Res 41:85–94. https://doi.org/10.1111/j.1600-079X.2006.00341.x

42. Fukuhara C, Yamazaki S, Liang J (2005) Pineal circadian clocks gate arylalkylamine N-acetyltransferase gene expression in the mouse pineal gland. J Neurochem 93:156–162. https://doi.org/10.1111/j.1471-4159.2004.03008.x

43. Jia C, Cheng C, Li T, Chen X, Yang Y, Liu X, Li S, Le W (2021) Alpha-synuclein up-regulates monoamine oxidase A expression and activity via trans-acting transcription factor 1. Front Aging Neurosci 13:653379. https://doi.org/10.3389/fnagi.2021.653379

44. Tanaka Y, Engelender S, Igarashi S, Rao RK, Wanner T, Tanzi RE, Sawa A, Dawson VL, Dawson, TM, Ross, CA (2001) Inducible expression of mutant alpha-synuclein decreases proteasome activity and increases sensitivity to mitochondria-dependent apoptosis. Hum Mol Genet 10:919–926. https://doi.org/10.1093/hmg/10.9.919

45. Chen L, Thiruchelvam MJ, Madura K, Richfield EK (2006) Proteasome dysfunction in aged human alpha-synuclein transgenic

mice. Neurobiol Dis 23:120–126. https://doi.org/10.1016/j.nbd.2006.02.004

46. Yan Y, Tao H, He J, Huang SY (2020) The HDOCK server for integrated protein-protein docking. Nat Protoc 15:1829–1852. https://doi.org/10.1038/s41596-020-0312-x

47. Chaudhuri KR, Schapira AH (2009) Non-motor symptoms of Parkinson's disease: dopaminergic pathophysiology and treatment. Lancet Neurol 8:464–474. https://doi.org/10.1016/S1474-4422(09)70068-7

48. Peever J, Fuller PM (2017) The biology of REM sleep. Curr Biol 27:R1237–R1248. https://doi.org/10.1016/j.cub.2017.10.026

49. Simor P, van der Wijk G, Nobili L, Peigneux P (2020) The microstructure of REM sleep: why phasic and tonic? Sleep Med Rev 52:101305. https://doi.org/10.1016/j.smrv.2020.101305

50. Lerner AB, Case JD, Takahashi Y (1960) Isolation of melatonin and 5-methoxyindole-3-acetic acid from bovine pineal glands. J Biol Chem 235:1992–1997

51. Li T, Cheng C, Jia C, Leng Y, Qian J, Yu H, Liu Y, Wang N, Yang Y, Al-Nusaif M, Le W (2021) Peripheral clock system abnormalities in patients with Parkinson's disease. Front Aging Neurosci 13:736026. https://doi.org/10.3389/fnagi.2021.736026

52. Marqueze EC, Nogueira LFR, Vetter C, Skene DJ, Cipolla-Neto J, Moreno CRC (2021) Exogenous melatonin decreases circadian misalignment and body weight among early types. J Pineal Res 71:e12750. https://doi.org/10.1111/jpi.12750

53. Sletten TL, Magee M, Murray JM, Gordon CJ, Lovato N, Kennaway DJ, Gwini SM, Bartlett DJ, Lockley SW, Lack LC, Grunstein RR, Rajaratnam SMW, Delayed Sleep on Melatonin Study (2018) Efficacy of melatonin with behavioural sleep-wake scheduling for delayed sleep-wake phase disorder: a double-blind, randomised clinical trial. PLoS Med 15:e1002587. https://doi.org/10.1371/journal.pmed.1002587

54. Kunz D, Stotz S, Bes F (2021) Treatment of isolated REM sleep behavior disorder using melatonin as a chronobiotic. J Pineal Res 71:e12759. https://doi.org/10.1111/jpi.12759

55. Pandi-Perumal SR, Trakht I, Srinivasan V, Spence DW, Maestroni GJ, Zisapel N, Cardinali DP (2008) Physiological effects of melatonin: role of melatonin receptors and signal transduction pathways. Prog Neurobiol 85:335–353. https://doi.org/10.1016/j.pneurobio.2008.04.001

56. Gobbi G, Comai S (2019) Sleep well Untangling the role of melatonin MT1 and MT2 receptors in sleep. J Pineal Res 66:12544. https://doi.org/10.1111/jpi.12544

57. Ochoa-Sanchez R, Comai S, Lacoste B, Bambico FR, Dominguez-Lopez S, Spadoni G, Rivara S, Bedini A, Angeloni D, Fraschini F, Mor M, Tarzia G, Descarries L, Gobbi G (2011) Promotion of non-rapid eye movement sleep and activation of reticular thalamic neurons by a novel MT2 melatonin receptor ligand. J Neurosci 31:18439–18452. https://doi.org/10.1523/JNEUROSCI.2676-11.2011

58. Gobbi G, Comai S (2019) Differential function of melatonin MT(1) and MT(2) receptors in REM and NREM sleep. Front Endocrinol (Lausanne) 10:87. https://doi.org/10.3389/fendo.2019.00087

59. Ochoa-Sanchez R, Comai S, Spadoni G, Bedini A, Tarzia G, Gobbi G (2014) Melatonin, selective and non-selective MT1/MT2 receptors agonists: differential effects on the 24-h vigilance states. Neurosci Lett 561:156–161. https://doi.org/10.1016/j.neulet.2013.12.069

60. Comai S, Ochoa-Sanchez R, Gobbi G (2013) Sleep-wake characterization of double MT(1)/MT(2) receptor knockout mice and comparison with MT(1) and MT(2) receptor knockout mice. Behav Brain Res 243:231–238. https://doi.org/10.1016/j.bbr.2013.01.008

61. Hu X, Li J, Wang X, Liu H, Wang T, Lin Z, Xiong N (2023) Neuroprotective effect of melatonin on sleep disorders Associated with Parkinson's disease. Antioxidants (Basel, Switzerland) 12:396. https://doi.org/10.3390/antiox12020396

62. Dauvilliers Y, Jennum P, Plazzi G (2013) Rapid eye movement sleep behavior disorder and rapid eye movement sleep without atonia in narcolepsy. Sleep Med 14:775–781. https://doi.org/10.1016/j.sleep.2012.10.006

63. Brooks PL, Peever JH (2011) Impaired GABA and glycine transmission triggers cardinal features of rapid eye movement sleep behavior disorder in mice. J Neurosci 31:7111–7121. https://doi.org/10.1523/JNEUROSCI.0347-11.2011

64. Matsuo K, Yabuki Y, Melki R, Bousset L, Owada Y, Fukunaga K (2021) Crucial role of FABP3 in alphaSyn-induced reduction of septal gabaergic neurons and cognitive decline in mice. Int J Mol Sci 22:400. https://doi.org/10.3390/ijms22010400

65. Shkodina AD, Tan SC, Hasan MM, Abdelgawad M, Chopra H, Bilal M, Boiko DI, Tarianyk KA, Alexiou A (2022) Roles of clock genes in the pathogenesis of Parkinson's disease. Ageing Res Rev 74:101554. https://doi.org/10.1016/j.arr.2021.101554

66. McKinnon C, De Snoo ML, Gondard E, Neudorfer C, Chau H, Ngana SG, O'Hara DM, Brotchie JM, Koprich JB, Lozano AM, Kalia LV, Kalia SK (2020) Early-onset impairment of the ubiquitin-proteasome system in dopaminergic neurons caused by alpha-synuclein. Acta Neuropathol Commun 8:17. https://doi.org/10.1186/s40478-020-0894-0

67. Karabiyik FR, C, Park SJ, Pavel M, Rubinsztein DC. (2021) Autophagy in ageing and ageing-related neurodegenerative diseases. Ageing Neur Dis 1:2

68. Johansen T, Lamark T (2011) Selective autophagy mediated by autophagic adapter proteins. Autophagy 7:279–296. https://doi.org/10.4161/auto.7.3.14487

69. Dehay B, Bove J, Rodriguez-Muela N, Perier C, Recasens A, Boya P, Vila M (2010) Pathogenic lysosomal depletion in Parkinson's disease. J Neurosci 30:12535–12544. https://doi.org/10.1523/JNEUROSCI.1920-10.2010

70. Koch JC, Bitow F, Haack J, d'Hedouville Z, Zhang JN, Tonges L, Michel U, Oliveira LM, Jovin TM, Liman J, Tatenhorst L, Bahr M, Lingor P (2015) Alpha-Synuclein affects neurite morphology, autophagy, vesicle transport and axonal degeneration in CNS neurons. Cell Death Dis 6:e1811. https://doi.org/10.1038/cddis.2015.169